Feasibility of using marine sediments in SCC pastes as supplementary cementitious materials

Amine El Mahdi Safhi, Mahfoud Benzerzour, P. Rivard, Nor-Edine Abriak

Feasibility of Using Marine Sediments in SCC Pastes as Supplementary Cementitious Materials

Amine el Mahdi Safhi [(1) (2) (3) (*)], **Mahfoud Benzerzour** [(1) (2)], **Patrice Rivard** [(3)], and **Nor-Edine Abriak** [(1) (2) (3)]

[(1)] IMT Lille Douai, Department of Civil Engineering and Environmental, Douai, 59500, France

[(2)] Université de Lille Nord de France, LGCgE, Villeneuve d'Ascq, 59650, France

[(3)] Université de Sherbrooke, Department of Civil and Building Engineering, Sherbrooke, QC J1K 2R1, Canada

Abstract

In the context of the depletion of natural geomaterials, the increasing amount of dredged sediments calls for seeking new possibilities for treating and recycling these materials as cementitious supplementary materials. The aim of this paper is to design ecological SCC pastes, which require less cement, incorporating treated marine sediments. Despite many approaches investigating the ultimate formula of self-compacting concrete (SCC), the process remains complex because it is based on many variables and components. According to the mix design method, twenty pastes were prepared with cement, superplasticizer, water, and treated marine sediments from the Dunkirk harbour (France). The pastes' fresh properties were determined by using the mini-slump cone (workability), and the Marsh cone (fluidity). Rheological properties were determined with a robust rheometer based on the Bingham model. Cohesiveness and compressive strength were tested as well. All responses were connected using ternary diagrams, which led to the definition of an optimal formula. Experimental checking was performed to validate the obtained results.

Keywords: Sediments; Mix design; Rheology; Recycling; Cohesiveness; SCC pastes

(*)Corresponding author: Amine el Mahdi Safhi

Email: amine.el.mahdi.safhi@usherbrooke.ca

Actual address: Université de Sherbrooke - Faculté de Génie – Department of Civil and Building Engineering

2500, boulevard de l'Université, Sherbrooke (Québec) J1K 2R1, Canada

1. Introduction

In a vision of sustainability, and to limit the depletion of natural resources, reduce CO_2 emissions, and strengthen biodiversity, the adoption of the circular economy as a model of consumption has become a major necessity. Dredged sediments could be an alternative additive in concrete, as well as a new source of construction materials. Sediments have been considered as waste materials for a long time [1]. However, when subjected to particular treatment, they have been demonstrated to have pozzolanic properties that may allow them to be used with Portland cement as a reactive or a simple mineral additive in the production of concrete [2,3]. Dredged sediments can be regarded as a suitable alternative for greener concrete structures.

The type of cement, the presence of additives, the water-to-cement ratio, the different types of admixtures, the dosages, the type and the size of aggregates are some of the factors that determine the final quality of concrete. However, a suitable mix design is not enough to achieve the expected properties. Fresh concrete must have rheological properties allowing it to properly fill the space in the workform between the rebars with the lowest segregation. High workability and good rheological stability are required for concrete. That is why concrete must meet very strict performance requirements to ensure the expected service life of any structure, especially for reinforced concrete elements, where the use of self-compacting concrete (SCC) is increasing.

SCC is a very fluid material, homogeneous and stable, that perfectly fits the shapes of the most complex forms. It was designed by Okamura in Japan for the purpose of facilitating casting in pieces of complex geometry, or located in inaccessible areas set up under their own weight without vibration. Different approaches to mix design have been proposed in previous studies [4] such as:

- The empirical design method: Okamura proposed an empirical method based on laboratory tests by fixing different ranges for each component in the SCC concrete [5]. Khaleel and Abdul Razak proposed an empirical method for SCC based on metakaolin and coarse aggregates with different properties. Using this method, they found that metakaolin enhances the SCC properties [6].

- The compressive strength method: Kheder and Al Jadiri proposed a method based on targeting a range of compressive strength by varying the water-to-cement ratio [7]. Dinakar et al. proposed a method started by fixing the total powder content; based on the required strength, the other parameters like W/C and fresh properties were then evaluated to meet the self-compactibility criteria [8].
- The close aggregate packing method: Kanadasan and Razak proposed to use the particles packing concept to secure the fresh and the hardened properties of SCC [9]. This method helped to promote sustainability by incorporating palm oil clinker aggregate. Sebaibi et al. proposed a method based on optimizing the SCC concrete using RENE LCPC software [10].
- The mixture design method based on the statistical factorial method: Bouziani developed a simplex-lattice mixture design with different factors and levels [11]. This study confirms that this approach is valid for a wide range of mixture proportions. Ozbay et al. used Taguchi's experiment design by using different factors [12]. This study analyzed the mixture proportion parameters of a high-strength SCC and it shows that the laboratory tests can be reproduced in a full-scale production.
- The mixture design method based on the rheology of the paste model: Ferrara et al. proposed a method for formulating a steel fibre-reinforced SCC based on developing a rheological model for pastes [13]. The model proved to be an efficient tool for the optimization of the SCC mixture.

Recently, studies have been focusing on the rheological understanding of this material and it has been reported that the control of the rheological properties is fundamental to optimize the SCC [14–16]. The rheological properties depend on many factors such as: the packing density, the specific surface area, water content, and film thicknesses [17–21]. Other studies show that the main factors influencing the rheology are the water-to-powder ratio and the superplasticizer dosage [22,23]. Despite previous studies investigate if those parameters influence individually or jointly the rheology of cementitious paste, it is still difficult to tell [24].

Rheological models are mathematical tools used to characterize the behaviour of a material during flowing. The choice of a model is determined by the type of material, as well as the rate of deformation the material is subjected to. Many rheological models have been proposed for the cementitious matrix since the beginning of the rheology study [25,26], especially for the cementitious matrix [27,28].

The rheology of SCC can be described with the Bingham or Herschel–Bulkley model [22]. In this paper, the Bingham model is considered to be the most appropriate. It includes three intrinsic parameters (τ_0, k, η) that describe the steady-state flow of the material in a homogeneous condition (no particle segregation). The shear stress τ (Pa) is then related to the shear rate $\dot{\gamma}$ (s^{-1}) using Eq. 1:

$$\tau = \tau_0 + \eta.\dot{\gamma} \qquad \textit{Eq. 1}$$

where τ_0 is the shear threshold of the material and η is the viscosity (Pa.s). Although some studies on SCC used the rheological Herschel–Bulkley model, some others demonstrated that the rheological model of Bingham is the most adaptable for use in the field of cementitious matrix [29–31]. The volume of the paste in SCC is much higher than in ordinary concrete, which leads to the use of more additives and admixtures. The composition of the paste is the main parameter affecting the self-compactibility properties [32].

The purpose of this work is to incorporate treated sediments as a replacement for Portland cement, and to evaluate their influence on the rheological behaviour of the mixture, which will have good environmental and economic benefits. This study is a part of a wider project on recycling sediments in SCC. This experimental study indicated that the volumetric amount of sediments in the mixtures can reach up to 14%, in other words, up to a sediments-to-cement-ratio of 0.29 in mass.

2. Materials and methods

2.1. Test equipment

The morphology of the treated sediments was analyzed using a Scanning Electron Microscope (SEM) Hitachi S-4700. The thermogravimetric analysis (TGA) was carried out with an

apparatus NETZSCH STA 449 using nitrogen gas in a controlled environment with argon flow (75 ml/min) at variable temperatures (105 °C to 1100 °C, ramp rate = 2 °C/min).

A mini-slump test developed by Kantro [33], with the proportional dimensions of the standard slump test cone was used to determine the workability. Strong correlations between this test and the apparent viscosity [34,35], and, in certain cases, with the yield stress have been reported previously [36,37]. The fluidity and the consistency were determined with a 10-mm orifice Marsh cone. The outflow time through the cone was measured to fill 1000 ml.

A Vicat apparatus was used to determine the water demand of the sediments. It is equipped with a consistency probe of 10 mm in diameter, as described in NF EN 196-3 standard [38].

For the rheological analysis, a robust Anton Paar Modular Compact Rheometer MCR 102 (Fig. 1) was used with a plane geometry. The shear rate varied from 1 to 100 s^{-1}.

Fig. 1. Anton Paar Modular Compact Rheometer MCR 102

2.2. Material properties

The cement used in this study is an Ordinary Portland Cement (OPC) CEM I 52.5 N (standard NF EN 197-1 [39]). This cement is communally used in studies about recycling sub-products because it contains no admixtures, in order to measure the real effect of the sediments. The sediments were dredged from *Grand Port Maritime de Dunkerque* (GPMD), located in the North of France. The raw sediments were heated at 850°C for 1 hour, after having been crushed and sieved through 120 μm sieves [3] (Fig. 2). This technique was very efficient to eliminate the high-water content and organic matter, and to modify the mineralogy and the composition of the raw sediments. The physical properties of the powders are shown in Fig. 2. Process of treatment (from left to right: sediment after drying, after grinding, after thermal treatment)

Table 1. The distribution of particles is given in Fig. 3. X-ray fluorescence (XRF) analysis was performed on the cement, and on the raw and treated sediments. The results are provided in Table 2. One can note that the concentration of most of the oxides increased in the sediments after the treatment. Fig. 4 shows the mineralogical composition of the raw and treated sediments obtained from X-ray diffraction (XRD). Quartz (SiO_2) and calcite ($CaCO_3$) were found as the main phases for the raw sediments. The analysis also indicated some minor phases such as gypsum ($CaSO_4$, $2H_2O$), haematite (Fe_2O_3), natrosilite ($Na_2Si_2O_5$) and halite (NaCl). After treatment, quartz

(SiO_2), gehlenite (several forms), and anhydrite ($CaSO_4$) were found as the main phases. The analysis also indicated some minor phases such as haematite (Fe_2O_3), augite, gypsum, and microcline ($KAlSi_3O_8$).

The morphology of treated sediments is shown in Fig. 5Fig. 5, it was observed that it consist of fine angular particles. According to Fig. 6, EDX analysis confirms the XRD analysis and it shows that the mineralogical nature of treated sediments is mainly siliceous.

The demand of superplasticizer (S_P) was measured using two types. The S_P Chryso Fluid Optima 206 appears to be the most suitable and the saturation assay starts from 1.5 % of the S_P dry extract to the cement mass.

The TGA analysis was conducted on the raw sediments. The results are presented in Fig. 7 and it shows that:

- Between 30 and 120 °C: the free water and some of the adsorbed water escape from the material. Unbound water is completely removed at 120°C
- Between 130 and 170 °C: a double endothermic reaction can take place associated with the decomposition of gypsum ($CaSO_4.2H_2O$)
- Between 180 and about 300°C: the first stage of dehydration. The heat breaks the particles and pulls the inter-granular water molecules
- At about 250 and 370 °C: small endothermic peaks may be produced indicating decomposition and oxidation effects of metallic elements (haematite)
- Between 450 and 550 °C: decomposition of the organic matter and organic pollutants
- Around 570 °C: there is a structural transformation from quartz α to quartz β
- Between 600 and 700 °C: this is the second step in the decarbonation of calcite.
- Between 700 and 900 °C: a highly endothermic reaction due to the decomposition of limestone ($CaCO_3$) that releases carbon dioxide (CO_2) and calcium oxide (CaO)
- Above 1000 – 1400 °C: the material goes to the mud state

157 The analysis confirms the choice of the calcination temperature, which is above the optimum of
158 750°C.

159 *Fig. 2. Process of treatment (from left to right: sediment after drying, after grinding, after thermal*
160 *treatment)*

161 *Table 1. Physical properties of cement and sediments*

162 *Fig. 3. Particle size distribution of cement, raw and treated sediments*

163 *Table 2. Oxide composition of cement, raw and treated sediments using XRF (%)*

164 *Fig. 4. XRD analysis on raw and treated sediments*

165 *Fig. 5. Particle morphology of treated sediments (300 μm)*

166 *Fig. 6. Energy Dispersive X-ray (EDX) analysis of treated sediments*

167 *Fig. 7. TGA analysis on the raw sediments*

168 ## 3. Experimental protocols

169 ### 3.1. Packing density and water demand

170 Water demand consists in determining the mass of water M_w required to make the
171 cementitious paste go from the state of pellets to a state of homogeneous paste. Tests were carried
172 out on 350 g of cement using a standard kneader (described in standard NF EN 196-1 [40]) and the
173 Vicat apparatus. The optimisation of water demand was performed by using the Réne-LCPC, a
174 developed software by Sedran and Larrard [41], which is based on a mathematical model in order to
175 secure a maximum packing density of the skeleton. This model makes it possible to calculate the
176 theoretical compactness of any granular mixture, and the viscosity of any suspension at a given
177 concentration of this mixture, based on various material characteristics. Physically speaking, a
178 higher compactness refers to a minimum percentage of voids between solid grains.

Penetration measurements were performed for different water contents. The mass of water M_w required to obtain a height h = 6 mm can be determined by successive tests. In order to limit the number of tests, it is possible to interpolate M_w from two points (A & B) framing the normal consistency. However, in order to minimize the error, points A and B must fulfill the following conditions (Eq. 2):

Eq. 2
$$\begin{cases} H_B \geq 2\ mm \\ 0.25 \leq W/C \leq\ 0.4 \\ M_{WB} -\ M_{WA} \leq 5\ g \end{cases}$$

The compactness ∅ of the powder is then determined by Eq. 3:

Eq. 3
$$\emptyset = \frac{1000}{1000 + \rho_c \frac{M_W}{M_C}}$$

where ρ_C is the density of the cement, M_w and M_C are the total mass of water and cement, respectively. The theoretical compactness (∅) was calculated using the commercial software Réne-LCPC as it shown in Fig. 8. It represents that the amount of sediments up to 70% improve the density of the mixture which can be explained by the finesse of the marine sediments and their ability to fill into voids between the cement grains. The water demand for treated sediments was 0.4.

Fig. 8. Theoretical packing density of the mixtures using René-LCPC software

3.2. Experimental design

The design of experiments (DoE) approach is based on a statistical method that can be used to optimize experimental tests. It is a well-known approach commonly used for the optimization of cementitious mixtures [42–45]. It allows the measurement of multiple responses without extra experiments. In our case, DoE allows us to quantify the influence of each mix parameter on the fresh properties of the mixtures. Furthermore, the responses depend only on the proportions of the compositions in the mixture and not on the mass or the volume.

The main characteristic of a random mixture is that the sum of all the components must be equal to 1. The experimental plan was based on four factors: cement (C), sediments (S), water (W), and superplasticizer (S_P) taken in volumetric proportion. With a total volume equal to unity, the mix design implies that there is an interaction and dependence between the parameters. The experimental field was constrained by Eq. 4:

$$Eq.\ 4 \qquad \sum_{i=1}^{i=n} x_i = C + S + W + Sp = 1$$

However, another important parameter was taken into consideration, namely the solid volumetric concentration (Γ). This is the ratio of the volume of solids to the total volume, which comprises the solid particles coming from cement, sediments, and superplasticizer in dry extract. This parameter is known to correlate with the yielded value [46]. It also correlates with the viscosity [47], which increases with the increase of the volume fraction of solids. This fact is valid only at a low shear rate and shear stress and for a $\Gamma_{max} = 0.62$ [48]. This limitation was confirmed elsewhere [49]. It was recommended to keep the volume ratio below 0.60 to avoid resistance against shear stress increase with the shear rate.

The mathematical model for this mix design converges toward a 2nd degree polynomial (Eq. 5), which can be written in a matrix form (Eq. 7) as the following:

$$Eq.\ 5 \qquad Y = \sum_{i=j}^{k} \beta_i x_j + \sum_{i<j} \sum_j \beta_{ij} x_i x_j + \varepsilon$$

$$Eq.\ 6 \qquad [Y] = [X].[\beta] + [\varepsilon]$$

where Y is the response, x_i and x_j correspond to the volumetric proportions of the mix factors, and β_i and β_{ij} are the regression coefficients. This model is known as the Scheffé canonical polynomials, widely used in mixture experiment applications [50,51]. This equation can be expanded to (Eq. 7):

$$Eq.\ 7 \qquad Y = \beta_1.C + \beta_2.S + \beta_3.W + \beta_4.SP + \beta_{12}.C.S + \beta_{13}.C.W + \beta_{23}.S.W + \beta_{14}.C.SP + \beta_{24}.C.Sp + \beta_{34}.W.Sp$$

where [X] is the experimental matrix, [β] is the vector of the model coefficients, and [ε] is the vector of the experimental error. After some preliminary tests in the laboratory, the range of variation of each component was as follows (Eq. 8):

$$\begin{cases} 0\,\% \le S \le 30\% \\ 0\,\% \le S_P \le 2\% \\ 0.25 \le W/C \le 0.4 \\ 0.57 \le \Gamma \le 0.59 \end{cases} \quad Eq.\ 8$$

Table 3 represents the range of variation of the different components.

Table 3. Implicit constraints

The field of study was a space of four dimensions, since there were four factors. The experimental matrix generated a hyper polyhedral. Numeric analysis was performed using a commercial software (Design Expert) dedicated for experimental mixture plans. The volume proportion of each component was calculated based on the given criteria.

3.3. Parametric study

The optimal experimental matrix was defined to achieve reliable and effective results. The dedicated software gives the mix proportions of a total of 20 points for modelling. Table 4 presents the determined arrangements of the 20 runs and their corresponding responses. Six mixtures were removed from the model design because they did not meet the criteria of self-compactibility (having a low workability and fluidity).

The water demand of the sediments was not considered in this arrangement. It was added separately for each mixture depending on the mass of sediments. The significance of the model (linear, quadratic, cubic, two-factor interaction, etc.), was investigated using robust software (Design-Expert and SPSS) and using the statistical model ANOVA (analysis of variances).

Table 4. Mix proportions and fresh properties of the mixtures

3.4. Preparation of specimens and Test methods

Mixture preparation was made according to NF EN 196-1 [40] procedure. Tests were conducted on fresh paste first. Using the mini slump flow diameter, the spreading out diameter (D_{flow}) was measured on a horizontal glass plate after 1 and 5 min to determine the workability. The fluidity and the consistency were determined using the Marsh cone. The outflow time (T_{flow}) was taken for 500 ml according to EN 445 standard [52]. The rheological analysis was performed between 5 and 7 min after starting the mixing operation.

The fresh pastes were poured in three 50-mm steel cubes, according to ASTM C 139 [53], and allowed to fill under its own weight. The specimens were removed from the moulds one day after casting, and were placed in curing water at a temperature of 20 ±2 °C. At 28 days, the compressive strength was measured in accordance with standard ASTM C109 [54].

Up to now there is no standard test method for evaluating the cohesiveness for a cementitious paste. However, Kwan has developed a protocol to measure this parameter using a mini version of the sieve segregation test [24,55]. The standard test consists in evaluating the sieve segregation index (SSI) by quantifying the portion of fresh SCC sample (4.8 ±0.2 kg) passing through a 5 mm sieve, from a height of 50 ±5 cm. Kwan suggested instead, to pour about 400 g of paste onto a 0.3 mm sieve from a height of 300 mm. In this study this protocol was used to measure the cohesiveness of the different pastes.

4. Results and discussion

The results of all the tests are presented in Table 5.

Table 5. Results of all the conducted tests

4.1. Workability

The results of the ANOVA analysis on the D_{flow} are provided in Table 6. This model is characterized by a R^2 of 0.923 and a predicted R^2 (0.844) in this case is in fair agreement with the adjusted R^2 (0.900). The Model F-value suggests that the model is significant. There is only a

0.01% chance that such F-value could occur due to noise. A p-value below 0.05 indicates that the model terms are significant. Values greater than 0.1 indicate that the model terms are not significant. The "Lack of Fit F-value" of 12.95 implies that the Lack of Fit is significant. There is only a 0.69% chance that such “Lack of Fit F-value” could occur due to noise.

Fig. 9 shows the slump flow responses in a ternary graph while fixing the cement proportion. For the same proportion of sediments (e.g. 0.112), the spread flow changes quickly from 140 to 185 mm, which means that the sediments have no effect on this parameter. The spread flow was not affected by the water content either; 180 mm could be obtained for a water range of variation between 0.41 and 0.43. The orientation of hatching confirms this fact. Again, the S_P content appears to be the dominant parameter in this ternary combination. According to Gomes [56] the value considered satisfactory for the flowing is 180 ±10 mm.

Table 6. ANOVA analyses of results for the D_{flow}

Fig. 9. The counter plots for slump flow (mm): 2D and 3D plot

4.2. Flowability

The linear model was a match for the flowability. The results of the ANOVA analysis on the T_{flow} are presented in Table 7. This model is characterized by a R^2 of 0.888 and a predicted R^2 (0.734) in this case is in fair agreement with the adjusted R^2 (0.854). The Model F-value suggests that the model is significant. There is only a 0.01 % chance that such F-value could occur due to noise. A p-value below 0.05 indicates that the model terms are significant. The "Lack of Fit F-value" of 4.72 implies a 5.69 % chance that a "Lack of Fit F-value" could occur due to noise, which is very low.

Fig. 10 shows the Marsh flow responses in a ternary graph while fixing the cement proportion (four components generate a cubic form that is hard to analyze). While all three variables affect the fluidity, the S_P content appears to be the dominant parameter in a ternary combination.

According to previous studies that used mini-slump and Marsh cones [57–60], good paste properties correspond to a $D_{flow} \geq 165$ mm and a $T_{flow} \leq 40$s, depending on the ratios of the concentration of solids to the total volume V_S/V_T, and of the volume of water to the total volume V_W/V_T.

Table 7. ANOVA analyses of results for the T_{flow}

Fig. 10. The counter plots for Marsh flow [s]: 2D and 3D plot

4.3. Rheological properties

The paste rheology was characterized using a rheometer and a plane geometry with variation of the shear rate ($\dot{\gamma}$) from 1 to 100 s^{-1}. The following properties were determined: yield stress (τ_0), shear stress (τ), and viscosity (η). The temperature was kept constant at 20±0.1 °C. The results fitted perfectly the Bingham model (Table 5) with a coefficient of determination $R^2 \geq 0.95$ as depicted in Fig. 11. This mixture can be characterized by a yield stress of 2.990 Pa and a viscosity of 1.163 Pa.s.

A correlation analysis was performed using the commercial software SPSS 24. Spearman's correlation coefficient ($\rho_{Spearman}$) was used to investigate the correlation between variables. The Spearman correlation is a non-parametric test that does not involve any assumptions about the distribution of the data.

Fig. 12 shows a moderate correlation between the V_W/V_C ratio and both viscosity and shear stress at a constant shear rate of 100 s^{-1}. The shear rate decreases with the increase of V_W/V_C ratio ($\rho_{Spearman}$= - 0.908), and the viscosity decreases with the increase of V_W/V_C ratio ($\rho_{Spearman}$= - 0.904).

A correlation analysis between both Marsh flow and yield point with the mini-slump flow is shown in Fig. 13. There is a strong relationship between both properties T_{flow} and D_{flow} ($\rho_{Spearman}$= - 0.913), a low flowability generates a high workability and vice-versa. There is also a strong correlation between D_{flow} and the yield point ($\rho_{Spearman}$= - 0.911).

Fig. 14 presents a correlation between both D_{flow} and T_{flow} with the V_W/V_C ratio. There is a strong relationship between the V_W/V_C ratio and the fresh properties. D_{flow} increases along with the V_W/V_C ratio ($\rho_{Spearman}$= 0.915), and the T_{flow} decreases while increasing the V_W/V_C ratio ($\rho_{Spearman}$= -0.943). It is found that the good results (low T_{flow} & high D_{flow}) are associated with a V_W/V_C ratio greater than 1.

Fig. 11. The data from the 2nd mix fitted perfectly the Bingham model

Fig. 12. Range of the variation of viscosity and shear stress corresponding to V_W/V_C variation

Fig. 13. Range of the variation of flowability and yield point corresponding to D_{flow}

Fig. 14. Range of the properties of the pastes corresponding to V_W/V_C variation

4.4. Cohesiveness

The sieve segregation index (SSI) for all the mixtures is presented in Table 5. A low SSI refers to a high cohesiveness and vice-versa. SSI were lower than 10 % as recommended [55], which ensure that the SCC pastes have a good stability as a coherent mass.

4.5. Paste strength

Results of the compressive strength tests conducted on the pastes specimens are shown in Table 5 and Fig. 15. The strength values are the average of three test specimens at the age of 28 days. As it is seen, the compressive strength varies from 78 to 101 MPa and by fixing cement percentage to 0.442%, strength varies from 83 to 87 MPa. Treated sediments generated a low reduction in compressive strength. However, from the orientation of hatching, the S_P content appears to be the dominant parameter in this ternary combination. The compressive strength increases with the increase of S_P content. Compared to the reference paste, a compressive strength of 85 MPa is required.

Fig. 15. The counter plots for compressive strength (MPa): 2D and 3D plot

5. Mixture optimization and validation of the model

The multi-criteria technique in Design-Expert allows us to set an optimization based on the overlay plots. The objective of this study is to maximize the mass of incorporated sediments while maintaining a good property of the pastes performances. Derringer and Suich [61] developed a global desirability function, represented in Eq. 9.

$$Eq.\ 9 \qquad D = (d_1^{r_1} \times d_2^{r_2} \times d_3^{r_3} \times \cdots \times d_n^{r_n})^{\frac{1}{\sum r_i}}$$

The combination of the different criteria is optimum for a D value close to 1. In Eq. 9, r_i is the relative importance assigned to the response *i*. It is a comparative scale of weighing each of the resulting d_i varying from 1 to 5. Goals can be assigned to the variables as to the responses and can be one of the following: maximize, minimize, target, or in the range. Table 8 provides the characterisation of the optimization function.

Fig. 16 shows the zone of desirability according to the overlay plot method. It suggests that the volumetric amount of sediments in the mixture can reach up to 14 %. Table 9 represents the optimal paste proportions according to both functions.

To assess the representability, repeatability, reproducibility, rapidity, and sensitivity of the model, a series of experiments were conducted with the optimal mixture proportions provided in Table 9. Table 10 shows the results with their absolute relative deviation (ARD) [42,51]. ARD is a parameter expressed in %, as in Eq. 10. It measures the predictability of the model and should not exceed 10%.

$$Eq.\ 10 \qquad ARD\ (\%) = \frac{Experimental - Model}{Experimental} \times 100$$

According to Table 10, the results of the ARD are in the desirable range (less than 10 %). The model is validated by the small difference between the theoretical and the experimental values. This experimental study indicated that the volumetric amount of sediments in the mixtures can reach up

364 to 14 %, in other words, sediments can replaces cement up to 0.29 as a sediments-to-cement-ratio,
365 0.30 as a water-to-cement-ratio, and 1.5 % of S_P dosage in the extract sec of cement mass.

366 *Table 8. Characterization of the desirability function*

367 *Fig. 16 . Overlay plot optimization following the proposed criteria*

368 *Table 9. Composition of the optimal pastes*

369 *Table 10. Absolute relative deviation of the predicted responses*

370 ## 6. Conclusion

371 The production of cement is a major concern to the industrial and scientific community. The
372 process of producing 1 ton of cement releases around 0.6 to 1.4 tons of CO_2 depending on the
373 process in each country [62–66]. The replacement of a part of the cement by treated sediments has a
374 major economic and environmental impact. Treated sediments can play a relevant role in
375 sustainability.

376 This paper focuses on the study of the effect of treated sediments on the rheological, fresh,
377 and hardened properties of SCC pastes. The results demonstrated that sediments can be used as a
378 supplementary cementitious material, with a volumetric amount up to 14 % (S/C = 0.29). At the
379 economical level, this result is very encouraging especially that the used sediments are naturally
380 available in large quantities and require less energy in the treatment comparing to the cement.

381 A mix design method based on the statistical mixture design approach was used in order to
382 evaluate the influence of each component of the mix. A numerical optimization efficiently
383 accomplished made it possible to design an SCC paste based on treated sediments. The statistical
384 analysis of the results highlighted the real relevance of the measured effects on the various factors,
385 as well as their interactions on the responses. The effects of the factors and their interactions were
386 more significant than the uncertainties.

The treated sediments improve the packing density of the cementitious materials. The empirical tests on fresh properties performed on the pastes correlate perfectly with the rheological parameters of the SCC pastes, namely the shear stress and the viscosity. The rheological tests performed less than 7 min after the start of mixing confirmed that the rheological behaviour of the pastes evolves from young ages.

The developed mini version of sieve segregation test is very promoting protocol that can be used as a foundation for a standardized test. Further research in this direction is suggested.

The use of different superplasticizers and viscosity agents may affect the repeatability of the results.

An extensive research is going on at our laboratories in order to evaluate the effect of entrained air and viscosity agent on a SCC mixture incorporating treated sediments.

Acknowledgements

This work was funded by the research funds of the IMT Lille Douai and grants from the Natural Sciences and Engineering Research Council of Canada (NSERC) and from the “Fonds de Recherche Nature et Technologies du Québec” (FRQNT).

References

[1] T.A. Dang, S. Kamali-Bernard, W.A. Prince, Design of new blended cement based on marine dredged sediment, Constr. Build. Mater. 41 (2013) 602–611. doi:10.1016/j.conbuildmat.2012.11.088.

[2] M. Amar, M. Benzerzour, N.-E. Abriak, Y. Mamindy-Pajany, Study of the pozzolanic activity of a dredged sediment from Dunkirk harbour, Powder Technol. 320 (2017) 748–764. doi:10.1016/j.powtec.2017.07.055.

[3] M. Amar, M. Benzerzour, A.E.M. Safhi, N.-E. Abriak, Durability of a cementitious matrix based on treated sediments, Case Stud. Constr. Mater. 8 (2018) 258–276. doi:10.1016/j.cscm.2018.01.007.

[4] C. Shi, Z. Wu, K. Lv, L. Wu, A review on mixture design methods for self-compacting concrete, Constr. Build. Mater. 84 (2015) 387–398. doi:10.1016/j.conbuildmat.2015.03.079.

[5] H. Okamura, Self-compacting high-performance concrete, Concr. Int. 19 (1997) 50–54.

413 [6] O.R. Khaleel, H. Abdul Razak, Mix design method for self compacting metakaolin concrete with
414 different properties of coarse aggregate, Mater. Des. 53 (2014) 691–700.
415 doi:10.1016/j.matdes.2013.07.072.
416 [7] G.F. Kheder, R.S. Al Jadiri, New Method for Proportioning Self-Consolidating Concrete Based on
417 Compressive Strength Requirements, ACI Mater. J. 107 (2010) 490–497.
418 [8] P. Dinakar, K.P. Sethy, U.C. Sahoo, Design of self-compacting concrete with ground granulated blast
419 furnace slag, Mater. Des. 43 (2013) 161–169. doi:10.1016/j.matdes.2012.06.049.
420 [9] J. Kanadasan, H.A. Razak, Mix design for self-compacting palm oil clinker concrete based on particle
421 packing, Mater. Des. 1980-2015. 56 (2014) 9–19. doi:10.1016/j.matdes.2013.10.086.
422 [10] N. Sebaibi, M. Benzerzour, Y. Sebaibi, N.-E. Abriak, Composition of self compacting concrete (SCC)
423 using the compressible packing model, the Chinese method and the European standard, Constr.
424 Build. Mater. 43 (2013) 382–388. doi:10.1016/j.conbuildmat.2013.02.028.
425 [11] T. Bouziani, Assessment of fresh properties and compressive strength of self-compacting concrete
426 made with different sand types by mixture design modelling approach, Constr. Build. Mater. 49
427 (2013) 308–314. doi:10.1016/j.conbuildmat.2013.08.039.
428 [12] E. Ozbay, A. Oztas, A. Baykasoglu, H. Ozbebek, Investigating mix proportions of high strength self
429 compacting concrete by using Taguchi method, Constr. Build. Mater. 23 (2009) 694–702.
430 doi:10.1016/j.conbuildmat.2008.02.014.
431 [13] L. Ferrara, Y.-D. Park, S.P. Shah, A method for mix-design of fiber-reinforced self-compacting
432 concrete, Cem. Concr. Res. 37 (2007) 957–971. doi:10.1016/j.cemconres.2007.03.014.
433 [14] N. Tregger, A. Gregori, L. Ferrara, S. Shah, Correlating dynamic segregation of self-consolidating
434 concrete to the slump-flow test, Constr. Build. Mater. 28 (2012) 499–505.
435 doi:10.1016/j.conbuildmat.2011.08.052.
436 [15] O.H. Wallevik, J.E. Wallevik, Rheology as a tool in concrete science: The use of rheographs and
437 workability boxes, Cem. Concr. Res. 41 (2011) 1279–1288. doi:10.1016/j.cemconres.2011.01.009.
438 [16] Q. Wu, X. An, Development of a mix design method for SCC based on the rheological characteristics
439 of paste, Constr. Build. Mater. 53 (2014) 642–651. doi:10.1016/j.conbuildmat.2013.12.008.

[17] L.G. Li, A.K.H. Kwan, Concrete mix design based on water film thickness and paste film thickness, Cem. Concr. Compos. 39 (2013) 33–42. doi:10.1016/j.cemconcomp.2013.03.021.

[18] R. Zhang, D.K. Panesar, New approach to calculate water film thickness and the correlation to the rheology of mortar and concrete containing reactive MgO, Constr. Build. Mater. 150 (2017) 892–902. doi:10.1016/j.conbuildmat.2017.05.218.

[19] X. Xie, T. Zhang, Y. Yang, Z. Lin, J. Wei, Q. Yu, Maximum paste coating thickness without voids clogging of pervious concrete and its relationship to the rheological properties of cement paste, Constr. Build. Mater. 168 (2018) 732–746. doi:10.1016/j.conbuildmat.2018.02.128.

[20] P.-L. Ng, A.K.-H. Kwan, L.G. Li, Packing and film thickness theories for the mix design of high-performance concrete, J. Zhejiang Univ.-Sci. A. 17 (2016) 759–781. doi:10.1631/jzus.A1600439.

[21] K.D. Kabagire, P. Diederich, A. Yahia, M. Chekired, Experimental assessment of the effect of particle characteristics on rheological properties of model mortar, Constr. Build. Mater. 151 (2017) 615–624. doi:10.1016/j.conbuildmat.2017.06.122.

[22] H. Li, F. Huang, Y. Xie, Z. Yi, Z. Wang, Effect of water–powder ratio on shear thickening response of SCC, Constr. Build. Mater. 131 (2017) 585–591. doi:10.1016/j.conbuildmat.2016.11.061.

[23] S. Grünewald, J.C. Walraven, Characteristics and influence of paste on the behaviour of self-compacting concrete in the fresh, in: 5th International RILEM Symposium on Self-Compacting Concrete, Ghent, Belgium, 2007: p. 6.

[24] J.J. Chen, W.W.S. Fung, A.K.H. Kwan, Effects of CSF on strength, rheology and cohesiveness of cement paste, Constr. Build. Mater. 35 (2012) 979–987. doi:10.1016/j.conbuildmat.2012.04.037.

[25] C. Atzeni, L. Massidda, U. Sanna, Comparison between rheological models for portland cement pastes, Cem. Concr. Res. 15 (1985) 511–519. doi:10.1016/0008-8846(85)90125-5.

[26] M. Nehdi, M.-A. Rahman, Estimating rheological properties of cement pastes using various rheological models for different test geometry, gap and surface friction, Cem. Concr. Res. 34 (2004) 1993–2007. doi:10.1016/j.cemconres.2004.02.020.

[27] V.K. Bui, Y. Akkaya, S.P. Shah, Rheological Model for Self-Consolidating Concrete, Mater. J. 99 (2002) 549–559. doi:10.14359/12364.

[28] A. Papo, Rheological models for cement pastes, Mater. Struct. 21 (1988) 41. doi:10.1007/BF02472527.

[29] F. Huang, H. Li, Z. Yi, Z. Wang, Y. Xie, The rheological properties of self-compacting concrete containing superplasticizer and air-entraining agent, Constr. Build. Mater. 166 (2018) 833–838. doi:10.1016/j.conbuildmat.2018.01.169.

[30] R.B. Singh, B. Singh, Rheological behaviour of different grades of self-compacting concrete containing recycled aggregates, Constr. Build. Mater. 161 (2018) 354–364. doi:10.1016/j.conbuildmat.2017.11.118.

[31] S. Girish, R.V. Ranganath, J. Vengala, Influence of powder and paste on flow properties of SCC, Constr. Build. Mater. 24 (2010) 2481–2488. doi:10.1016/j.conbuildmat.2010.06.008.

[32] A. Mebrouki, N. Belas, K. Bendani, N. Bouhamou, A Self-Compacting Cement Paste Formulation using Mixture Design, J. Appl. Sci. 9 (2009). doi:10.3923/jas.2009.4127.4136.

[33] D.L. Kantro, Influence of Water-Reducing Admixtures on Properties of Cement Paste—A Miniature Slump Test, Cem. Concr. Aggreg. 2 (1980) 95–102. doi:10.1520/CCA10190J.

[34] M. Cyr, Contribution à la caractérisation des fines minérales et à la compréhension de leur rôle joué dans le comportement rhéologique des matrices cimentaires, PhD Thesis, INSA de Toulouse; Université de Sherbrooke, 1999.

[35] J.E. Wallevik, Relationship between the Bingham parameters and slump, Cem. Concr. Res. 36 (2006) 1214–1221. doi:10.1016/j.cemconres.2006.03.001.

[36] C.F. Ferraris, K.H. Obla, R. Hill, The influence of mineral admixtures on the rheology of cement paste and concrete, Cem. Concr. Res. 31 (2001) 245–255. doi:10.1016/S0008-8846(00)00454-3.

[37] N. Roussel, C. Stefani, R. Leroy, From mini-cone test to Abrams cone test: measurement of cement-based materials yield stress using slump tests, Cem. Concr. Res. 35 (2005) 817–822. doi:10.1016/j.cemconres.2004.07.032.

[38] AFNOR, NF EN 196-3□: Méthodes d'essai des ciments - Partie 3□: détermination du temps de prise et de la stabilité, (2017).

[39] AFNOR, NF EN 197-1□: Ciment - Partie 1□: composition, spécifications et critères de conformité des ciments courants, (2012).

494 [40] AFNOR, NF EN 196-1□: Methods of testing cement — Part 1: Determination of strength, (2016).
495 [41] T. Sedran, F. De Larrard, L. Le Guen, Détermination de la compacité des ciments et additions
496 minérales à la sonde de Vicat, Bull. Lab. Ponts Chaussées. (2007) pp 155-163.
497 [42] S. Fatemi, M.K. Varkani, Z. Ranjbar, S. Bastani, Optimization of the water-based road-marking paint
498 by experimental design, mixture method, Prog. Org. Coat. 55 (2006) 337–344.
499 doi:10.1016/j.porgcoat.2006.01.006.
500 [43] S. Imanzadeh, A. Hibouche, A. Jarno, S. Taibi, Formulating and optimizing the compressive strength
501 of a raw earth concrete by mixture design, Constr. Build. Mater. 163 (2018) 149–159.
502 doi:10.1016/j.conbuildmat.2017.12.088.
503 [44] A.M. Matos, L. Maia, S. Nunes, P. Milheiro-Oliveira, Design of self-compacting high-performance
504 concrete: Study of mortar phase, Constr. Build. Mater. 167 (2018) 617–630.
505 doi:10.1016/j.conbuildmat.2018.02.053.
506 [45] S.M. Mirabedini, S.S. Jamali, M. Haghayegh, M. Sharifi, A.S. Mirabedini, R. Hashemi-Nasab,
507 Application of mixture experimental design to optimize formulation and performance of
508 thermoplastic road markings, Prog. Org. Coat. 75 (2012) 549–559.
509 doi:10.1016/j.porgcoat.2012.05.012.
510 [46] S.N. Ghosh, Advances in Cement Technology: Chemistry, Manufacture and Testing, CRC Press, 2003.
511 [47] H. Justnes, H. Vikan, Viscosity of cement slurries as a function of solids content, Ann Trans Nord.
512 Rheol. Soc. 13 (2005) 75–82.
513 [48] A. Nzihou, L. Attias, P. Sharrock, A. Ricard, A rheological, thermal and mechanical study of bone
514 cement—from a suspension to a solid biomaterial, Powder Technol. 99 (1998) 60–69.
515 doi:10.1016/S0032-5910(98)00091-6.
516 [49] W. Kurdowski, Cement and Concrete Chemistry, Springer Science & Business, 2014.
517 [50] H. Scheffé, Experiments With Mixtures, J. R. Stat. Soc. Ser. B Methodol. 20 (1958) 344–360.
518 [51] E. Ghafari, H. Costa, E. Júlio, Statistical mixture design approach for eco-efficient UHPC, Cem. Concr.
519 Compos. 55 (2015) 17–25. doi:10.1016/j.cemconcomp.2014.07.016.
520 [52] AFNOR, NF EN 445□: Coulis pour câble de précontrainte - Méthodes d'essai, (2007).

[53] ASTM, ASTM C139□: Standard Specification for Concrete Masonry Units for Construction of Catch Basins and Manholes, (2017).

[54] ASTM, ASTM C109 / C109M□: Standard Test Method for Compressive Strength of Hydraulic Cement Mortars (Using 2-in. or [50-mm] Cube Specimens), (2016).

[55] A.K.H. Kwan, J.-J. Chen, W.W.S. Fung, Effects of superplasticiser on rheology and cohesiveness of CSF cement paste, Adv. Cem. Res. 24 (2012) 125–137. doi:10.1680/adcr.10.00020.

[56] P. Gomes, Optimization and characterization of high-strength self-compacting concrete, Universitat Politècnica da Catalunya, 2002.

[57] S. Nunes, P.M. Oliveira, J.S. Coutinho, J. Figueiras, Rheological characterization of SCC mortars and pastes with changes induced by cement delivery, Cem. Concr. Compos. 33 (2011) 103–115. doi:10.1016/j.cemconcomp.2010.09.019.

[58] F. Soltanzadeh, J. Barros, R. Francisco, C. Santos, Steel fiber reinforced self-compacting concrete: from material to mechanical behavior table of contents, 2012.

[59] A. Basheerudeen, S. Anandan, Particle Packing Approach for Designing the Mortar Phase of Self Compacting Concrete, Eng. J. 18 (2014) 127–140. doi:10.4186/ej.2014.18.2.127.

[60] J.L. Calmon, F.A. Tristão, M. Giacometti, M. Meneguelli, M. Moratti, J.E.S.L. Teixeira, Effects of BOF steel slag and other cementitious materials on the rheological properties of self-compacting cement pastes, Constr. Build. Mater. 40 (2013) 1046–1053. doi:10.1016/j.conbuildmat.2012.11.039.

[61] G. Derringer, R. Suich, Simultaneous Optimization of Several Response Variables, J. Qual. Technol. 12 (1980) 214–219. doi:10.1080/00224065.1980.11980968.

[62] S. Licht, Co-production of cement and carbon nanotubes with a carbon negative footprint, J. CO_2 Util. 18 (2017) 378–389. doi:10.1016/j.jcou.2017.02.011.

[63] L.M. Vizcaíno-Andrés, S. Sánchez-Berriel, S. Damas-Carrera, A. Pérez-Hernández, K.L. Scrivener, J.F. Martirena-Hernández, Industrial trial to produce a low clinker, low carbon cement, Mater. Constr. 65 (2015) e045. doi:10.3989/mc.2015.00614.

546 [64] W. Shen, Y. Liu, B. Yan, J. Wang, P. He, C. Zhou, X. Huo, W. Zhang, G. Xu, Q. Ding, Cement industry
547 of China: Driving force, environment impact and sustainable development, Renew. Sustain. Energy
548 Rev. 75 (2017) 618–628. doi:10.1016/j.rser.2016.11.033.
549 [65] Z. Wei, B. Wang, G. Falzone, E.C. La Plante, M.U. Okoronkwo, Z. She, T. Oey, M. Balonis, N.
550 Neithalath, L. Pilon, G. Sant, Clinkering-free cementation by fly ash carbonation, J. CO2 Util. 23
551 (2018) 117–127. doi:10.1016/j.jcou.2017.11.005.
552 [66] D. Xu, Y. Cui, H. Li, K. Yang, W. Xu, Y. Chen, On the future of Chinese cement industry, Cem. Concr.
553 Res. 78 (2015) 2–13. doi:10.1016/j.cemconres.2015.06.012.
554

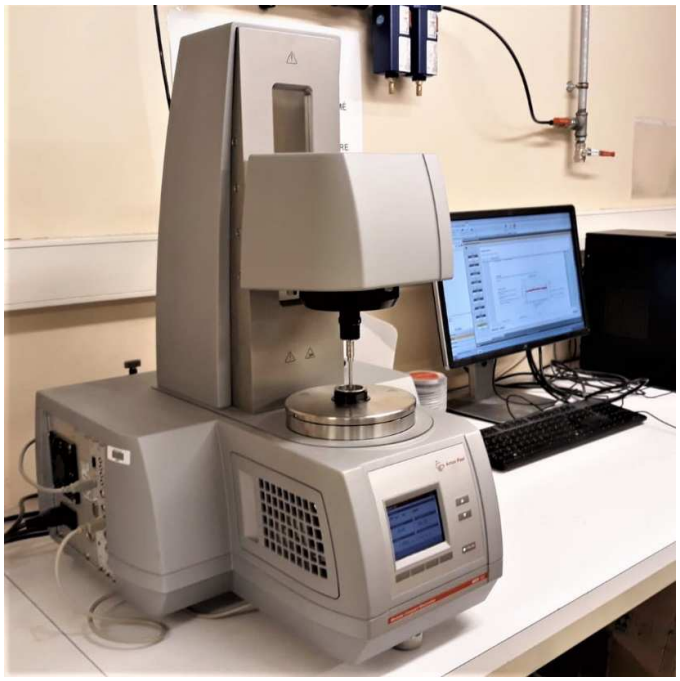

Fig. 1. Anton Paar Modular Compact Rheometer MCR 102

Fig. 2. Process of treatment (from left to right: sediment after drying, after grinding, after thermal treatment)

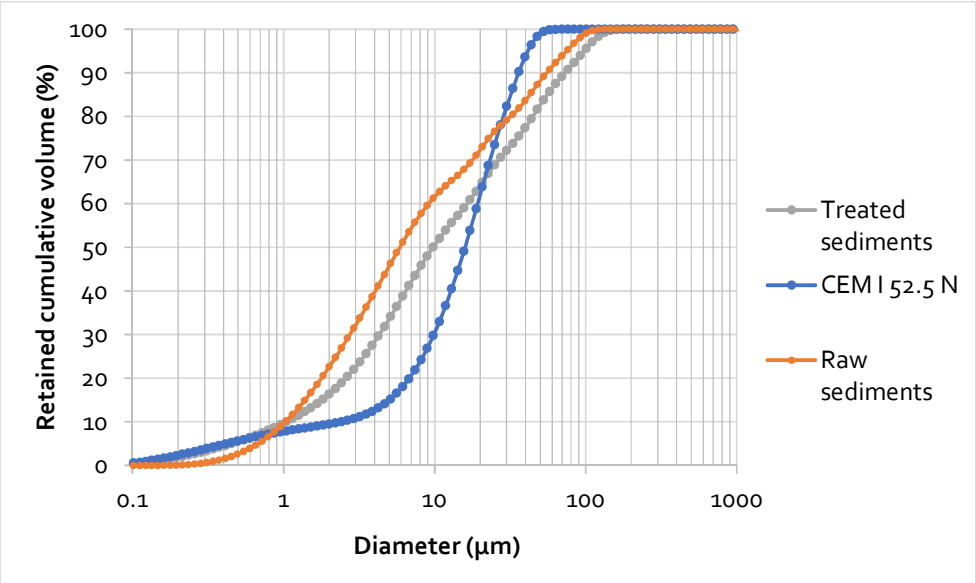

Fig. 3. Particle size distribution of cement, raw and treated sediments

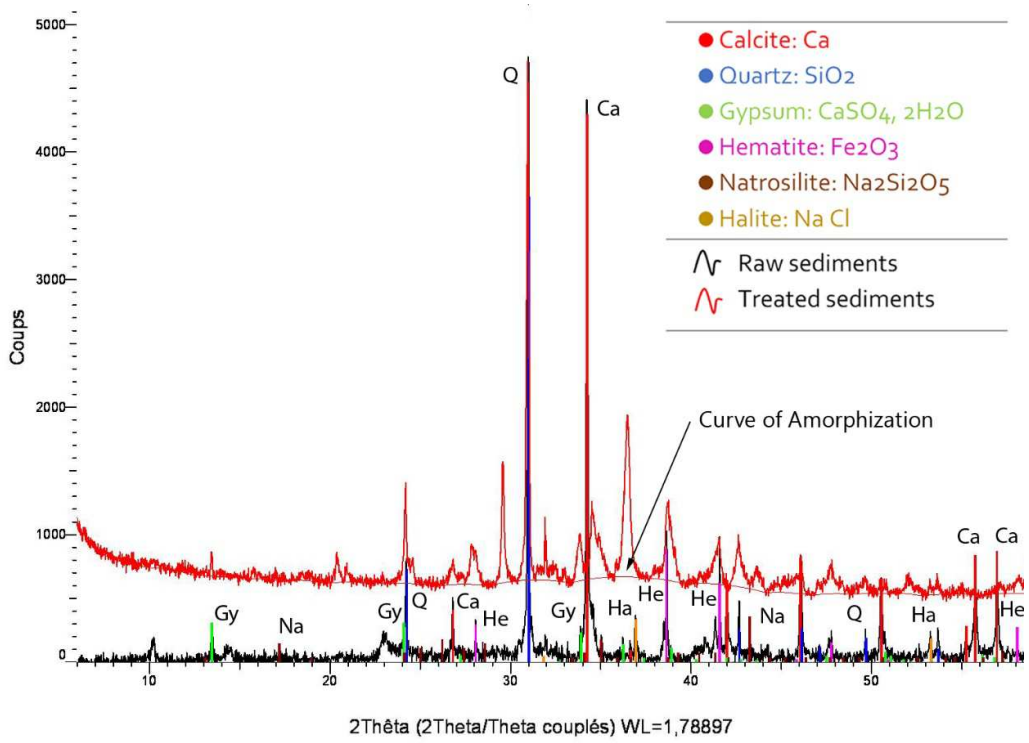

Fig. 4. XRD analysis on raw and treated sediments

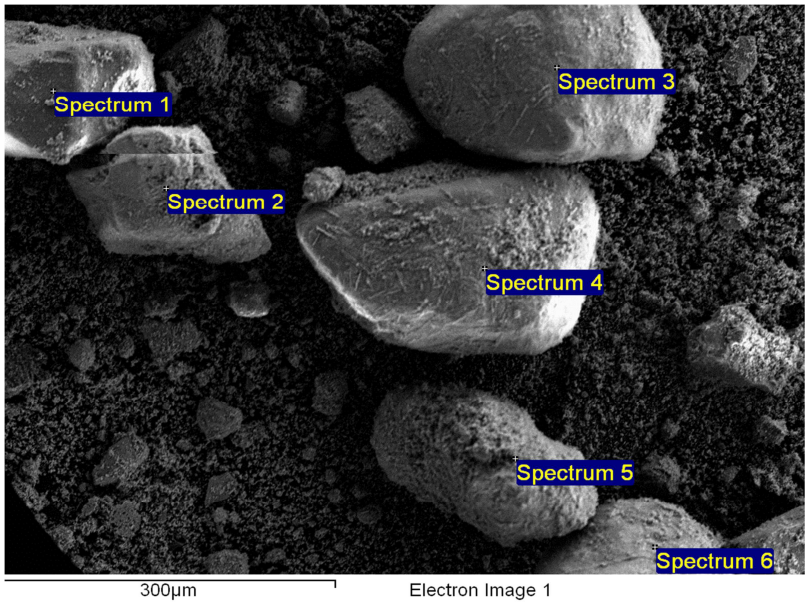

Fig. 5. Particle morphology of treated sediments (300 µm)

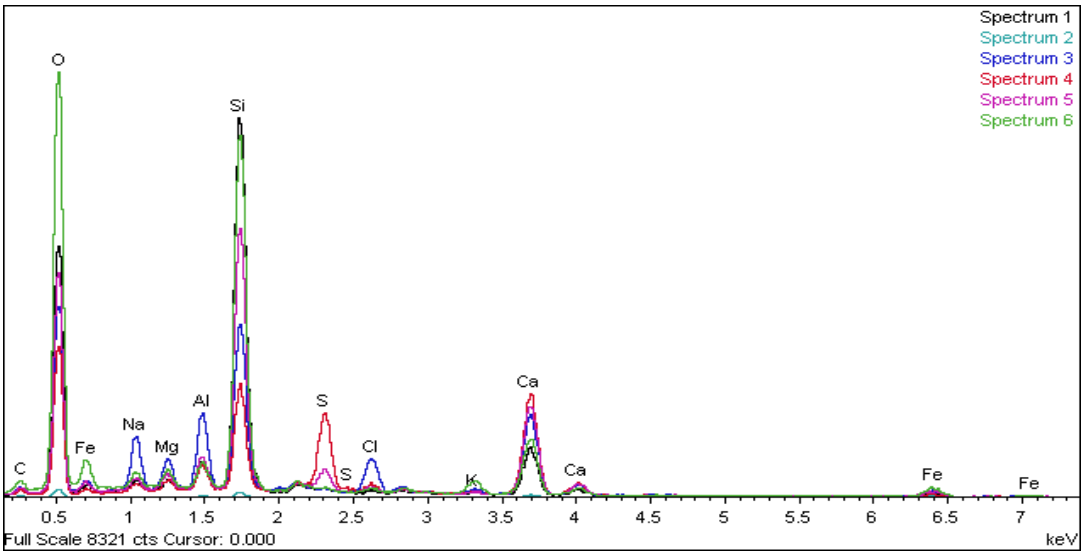

17

18 *Fig. 6. Energy Dispersive X-ray (EDX) analysis of treated sediments*

19

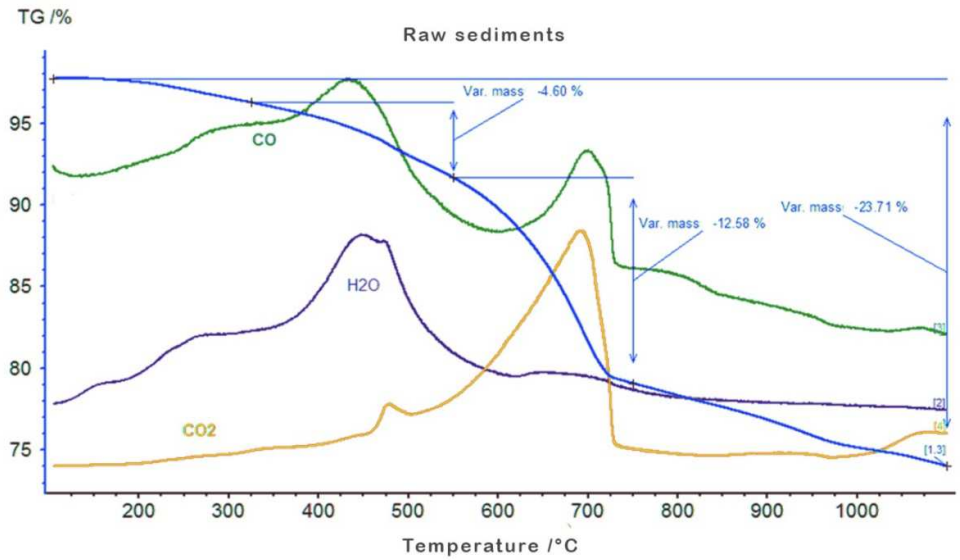

Fig. 7. TGA analysis on the raw sediments

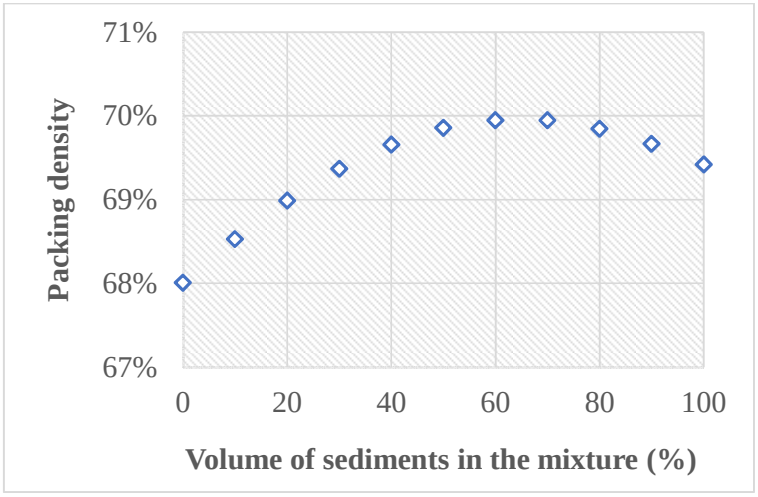

Fig. 8. Theoretical packing density of the mixtures using René-LCPC software

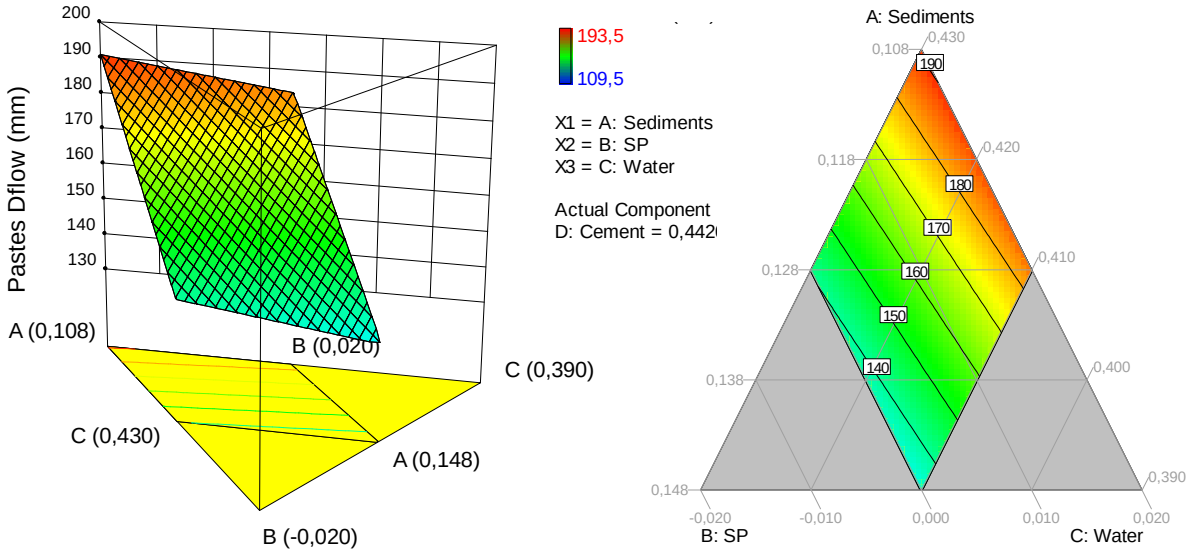

Fig. 9. The counter plots for slump flow (mm): 2D and 3D plot

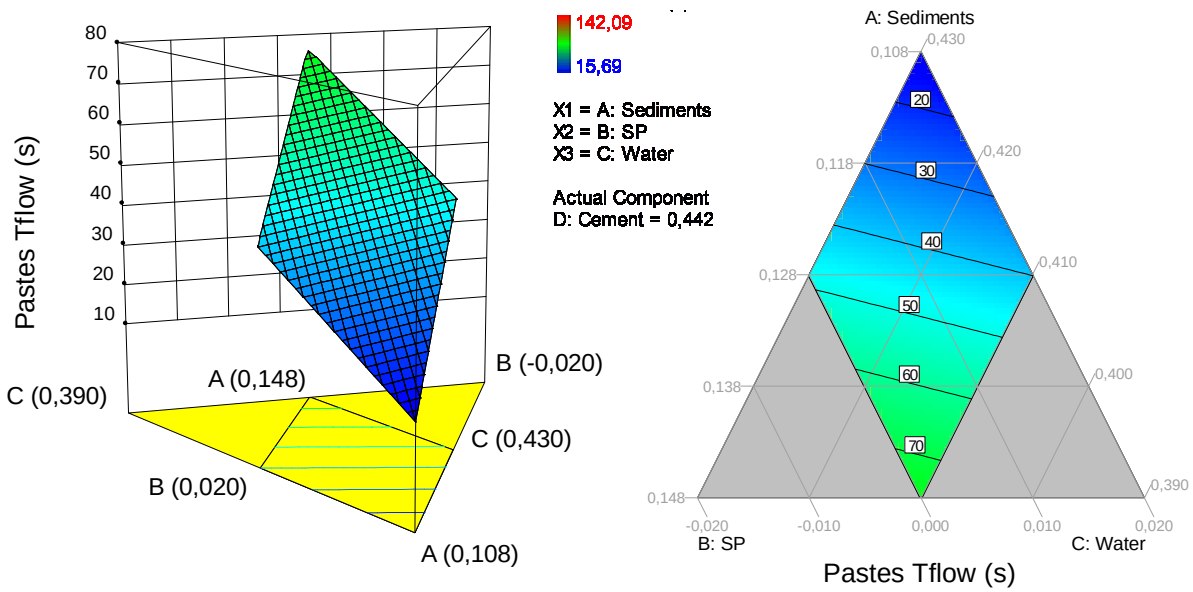

Fig. 10. The counter plots for Marsh flow [s]: 2D and 3D plot

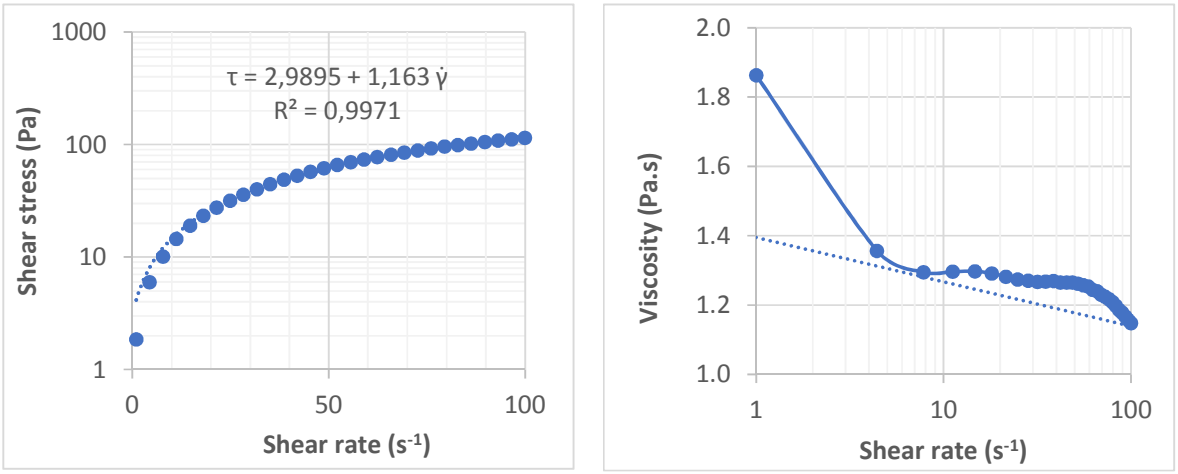

Fig. 11. The data from the 2nd mix fitted perfectly the Bingham model

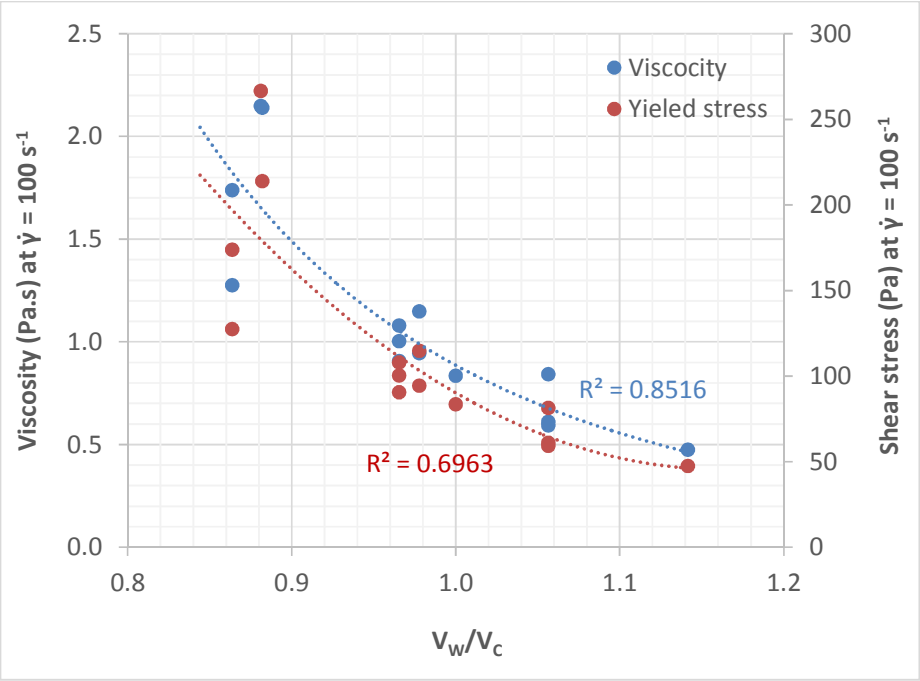

Fig. 12. Range of the variation of viscosity and shear stress corresponding to V_W/V_C variation

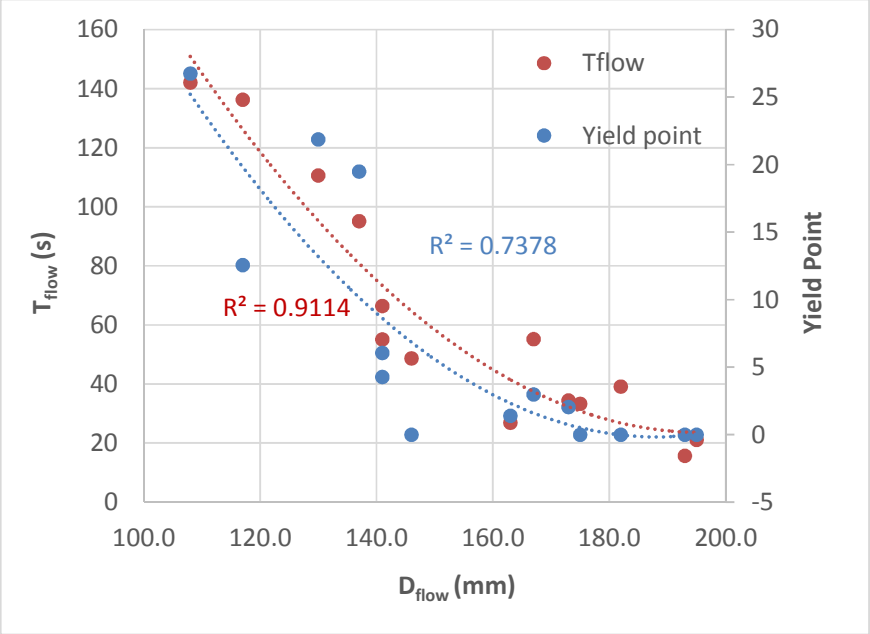

38

39 *Fig. 13. Range of the variation of flowability and yield point corresponding to D_{flow}*

40

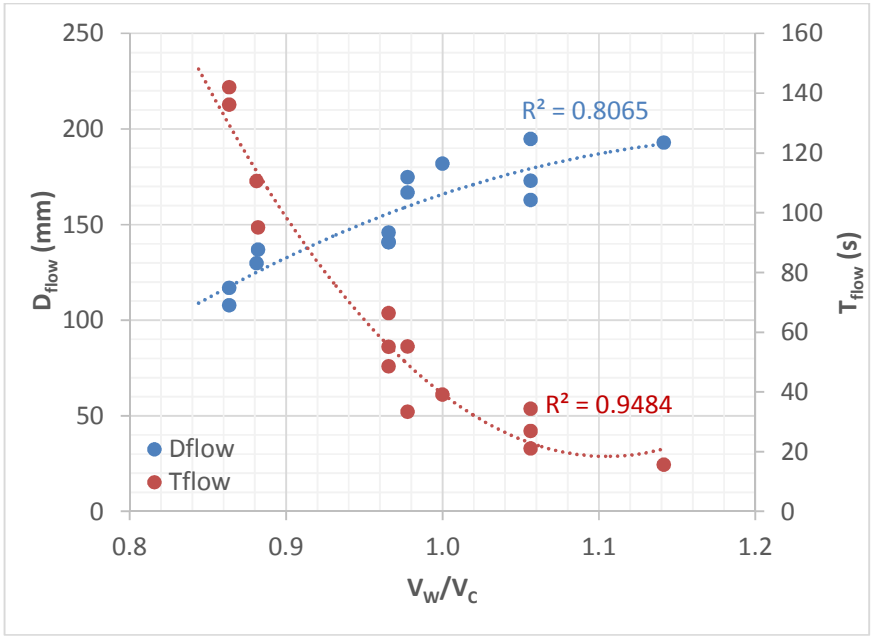

41

42 *Fig. 14. Range of the properties of the pastes corresponding to V_W/V_C variation*

43

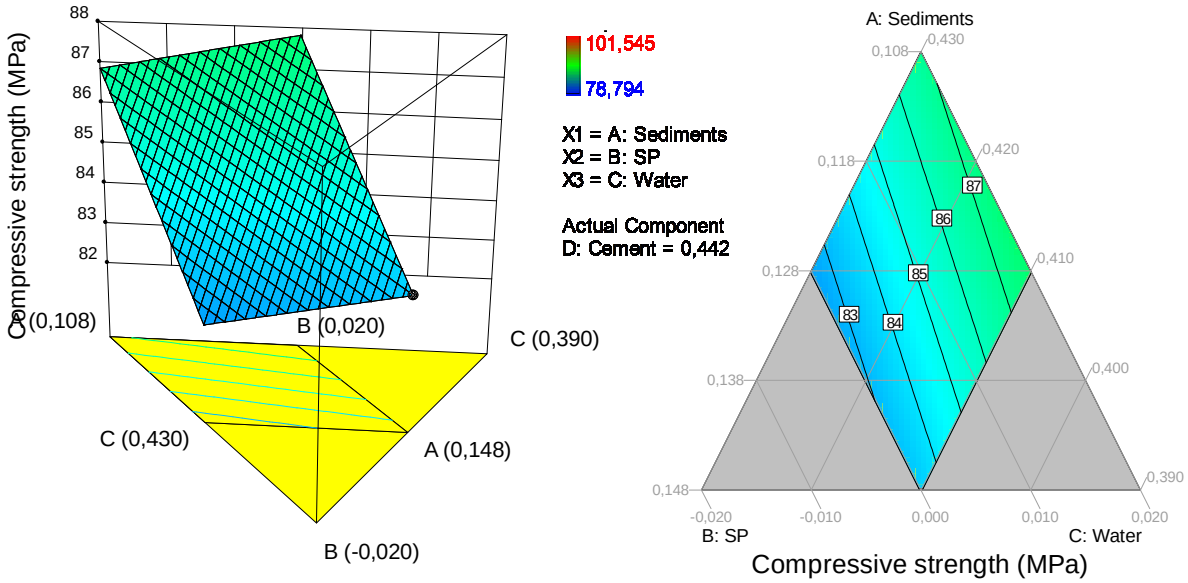

Fig. 15. The counter plots for compressive strength (MPa): 2D and 3D plot

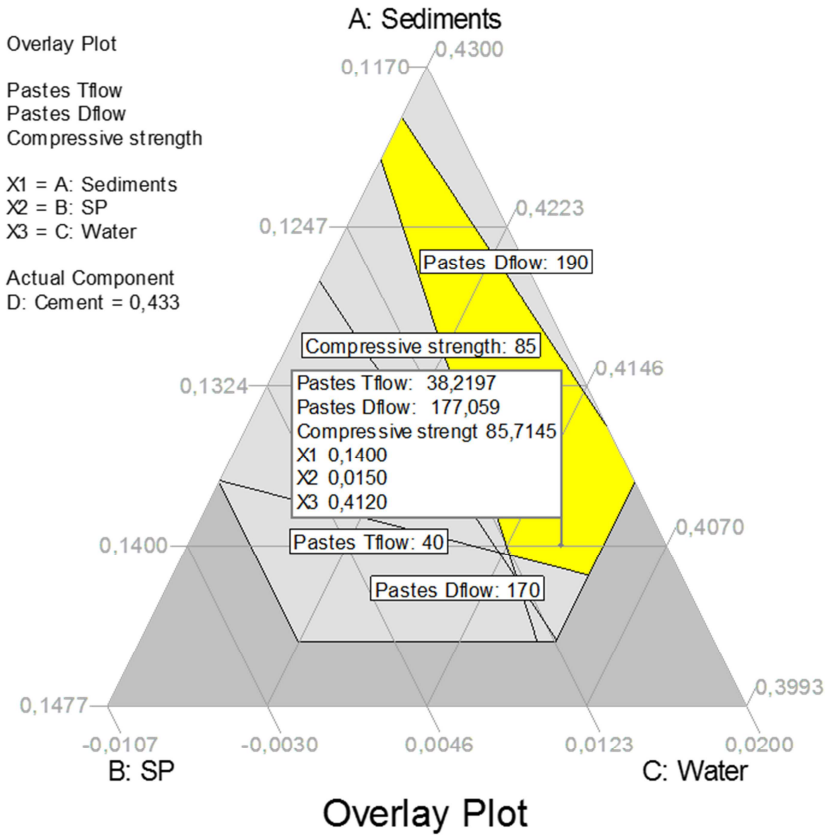

47

48 *Fig. 16 . Overlay plot optimization following the proposed criteria*

Table 1. Physical properties of cement and sediments

components	***Density (kg/m³)***	***Specific area BET (m²/kg)***	***Average diameter D_{50} (μm)***
Cement	3176	914	15.9
Raw sediments	2520	3652	5.90
Treated sediments	2851	2335	9.80

Table 2. Oxide composition of cement, raw and treated sediments using XRF (%)

Oxides composition	***Raw sediments***	***Treated sediments***	***CEM I 52.5 N***
SiO_2	38.8	36.4	17.3
Al_2O_3	11.0	10.1	5.41
MgO	2.69	2.62	1.23
Fe_2O_3	13.3	12.7	4.09
CaO	23.3	26.0	62.8
Na_2O	2.08	2.31	0.71
K_2O	2.08	1.65	0.76
P_2O_5	0.51	0.47	0.49
SO_3	4.37	5.43	4.49
TiO_2	0.54	0.51	0.35
MnO	0.17	0.18	Traces
ZnO	0.20	0.17	0.13

Table 3. Implicit constraints

Component volume	***S***	S_P	***E***	***C***
Coded	*A*	*B*	*C*	*D*
Lower constraints	0.009	0.000	0.410	0.412
Higher constraints	0.148	0.020	0.430	0.541

Table 4. Mix proportions and fresh properties of the mixtures

Run	Percentage of mixture volume				Relevant parameters				
	Sediments	S_P	Water	Cement	W/C	S/C	V_W/V_P	$S_P/C\%$	V_W/V_C
1	0.09	0.02	0.42	0.47	0.24	0.16	0.79	2.10	0.93
2	0.09	0.02	0.42	0.47	0.24	0.16	0.79	2.10	0.93
3	0.06	0.01	0.41	0.52	0.23	0.11	0.72	1.05	0.81
~~4~~	~~0.05~~	~~0.00~~	~~0.42~~	~~0.53~~	~~0.23~~	~~0.09~~	~~0.72~~	~~0.00~~	~~0.79~~
~~5~~	~~0.15~~	~~0.00~~	~~0.41~~	~~0.44~~	~~0.22~~	~~0.30~~	~~0.69~~	~~0.00~~	~~0.93~~
6	0.08	0.01	0.43	0.48	0.25	0.15	0.79	1.05	0.92
7	0.12	0.02	0.42	0.45	0.23	0.23	0.75	1.58	0.95
8	0.14	0.01	0.42	0.43	0.24	0.30	0.75	1.05	1.01
9	0.08	0.01	0.43	0.48	0.25	0.15	0.79	1.05	0.92
10	0.03	0.02	0.42	0.53	0.24	0.05	0.79	2.10	0.83
~~11~~	~~0.03~~	~~0.00~~	~~0.43~~	~~0.54~~	~~0.24~~	~~0.05~~	~~0.75~~	~~0.00~~	~~0.79~~
12	0.14	0.01	0.42	0.43	0.24	0.30	0.75	1.05	1.01
~~13~~	~~0.08~~	~~0.01~~	~~0.42~~	~~0.50~~	~~0.23~~	~~0.15~~	~~0.72~~	~~0.53~~	~~0.84~~
14	0.01	0.02	0.43	0.54	0.25	0.01	0.82	2.10	0.83
15	0.14	0.02	0.43	0.41	0.25	0.30	0.82	2.10	1.09
16	0.06	0.01	0.41	0.52	0.23	0.11	0.72	1.05	0.81
17	0.08	0.01	0.43	0.48	0.25	0.15	0.79	1.05	0.92
~~18~~	~~0.14~~	~~0.00~~	~~0.43~~	~~0.43~~	~~0.24~~	~~0.30~~	~~0.75~~	~~0.00~~	~~1.01~~
~~19~~	~~0.11~~	~~0.00~~	~~0.41~~	~~0.48~~	~~0.22~~	~~0.21~~	~~0.69~~	~~0.00~~	~~0.86~~
20	0.14	0.02	0.41	0.43	0.23	0.30	0.75	2.10	1.01

Table 5. Results of all the conducted tests

Mix N°	***Mini-slump diameter (mm)***		***March cone flow (s)***	***Yield point τ_0 (Pa)***	***Viscosity η (Pa.s)***	***ISS (%)***	***Dry weight (kg/m3)***	***Compressive strength (MPa) 28d***
	After 1 min	***After 5 min***						
1	175	182	33.38	0.007	0.964	4.4	2110	97.6
2	167	170	55.28	2.990	1.163	5.9	2116	94.8
3	117	118	136.3	12.57	1.183	4.4	2150	95.3
~~*4*~~	-	-	-	-	-	-	-	-
~~*5*~~	-	-	-	-	-	-	-	-
6	141	143	66.47	6.051	0.853	2.0	2118	96.8
7	182	185	39.13	0.003	0.839	5.9	2083	90.0
8	173	173	34.47	2.052	0.600	4.5	2092	83.1
9	141	142	55.16	4.285	0.973	1.2	2125	82.3
10	137	138	95.16	19.50	2.186	1.2	2170	82.4
~~*11*~~	-	-	-	-	-	-	-	-
12	163	164	26.94	1.395	0.586	0.8	2103	80.4
~~*13*~~	-	-	-	-	-	-	-	-
14	130	130	110.7	21.89	2.448	1.3	2187	99.9
15	193	195	15.69	0.007	0.460	9.8	2062	78.8
16	108	108	142.1	26.76	1.519	1.2	2106	90.5
17	146	146	48.68	0.007	1.052	1.8	2117	88.9
~~*18*~~	-	-	-	-	-	-	-	-
~~*19*~~	-	-	-	-	-	-	-	-
20	195	196	21.16	0.004	0.856	8.1	2085	87.5

16 *Table 6. ANOVA analyses of results for the D_{flow}*

Source	***Sum of Squares***	***df***	***Mean Square***	***F- Value***	***p-value Prob > F***
Model	8847	3	2949	40.06	< 0.0001
Linear Mixture	*8847*	*3*	*2949*	*40.06*	*< 0.0001*
Residual	736.2	10	73.62		
Lack of Fit	*683.4*	*5*	*136.7*	*12.95*	*0.0069*
Pure Error	*52.79*	*5*	*10.56*		

17

18

19 *Table 7. ANOVA analyses of results for the T_{flow}*

Source	***Sum of Squares***	***df***	***Mean Square***	***F-value***	***p-value Prob > F***
Model	20262	3	6754	26.41	< 0.0001
Linear Mixture	*20262*	*3*	*6754*	*26.41*	*< 0.0001*
Residual	2556	10	255.7		
Lack of Fit	*2110*	*5*	*422.0*	*4.72*	*0.0569*
Pure Error	*447.2*	*5*	*89.43*		

20

21

22 *Table 8. Characterization of the desirability function*

Response and variables	***lower***	***Upper***	***Criteria***
Workability (mm)	170	190	In range
Flowability (s)	15.6	40.0	In range
Cohesiveness (ISS %)	0.00	10.0	In range
Compressive strength (MPa)	85.0	99.9	In range

23

24

25 *Table 9. Composition of the optimal pastes*

Mixes	***Component***				***Relevant parameters***			
	C	***S***	***S_P*** [1]	***W*** [2]	***W/C***	***S/C***	***V_W/V_P***	***V_W/V_C***
Volume proportions (%)	0.433	0.140	0.015	0.412	0.30	0.29	0.75	1.00
Dosage (kg/m^3)	1375	399.2	15.00	412.0				

26

27

[1] In dry extract

[2] Plus the water demand of the sediments

28 *Table 10. Absolute relative deviation of the predicted responses*

Response and variables	***Theoretical values***	***Experimental values***	***ARD (%)***
Workability (mm)	177	174	4.1
Flowability (s)	38.2	34.7	9.5
Cohesiveness (ISS %)	7.55	7.12	6.0
Compressive strength (MPa)	85.7	81.2	5.5

29